VDI Entwicklung Konstruktion Vertrieb

Programme

October 7th/8th, 2002
in Munich/Germany, Forum Hotel

with exhibition

CVT 2002 Congress

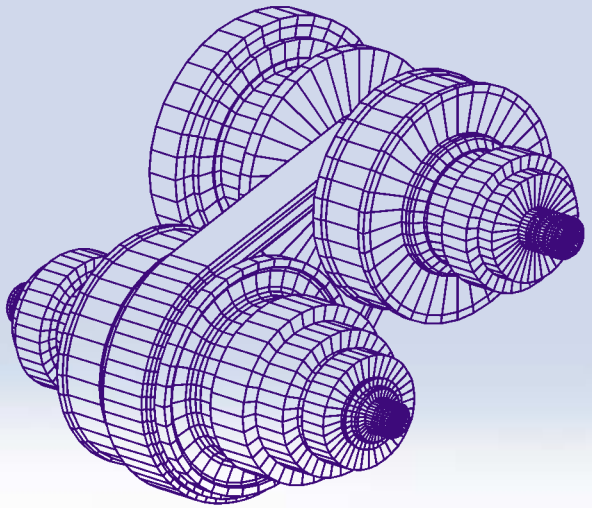

EXPERIMENTAL RESULTS FOR A TWO-MODE SPLIT-WAY CVT

Prof. Alberto Beccari, Dr. Marco Cammalleri and Prof. Francesco Sorge
Department of Mechanics and Aeronautics, University of Palermo
Viale delle Scienze, 90128 - Palermo, Italy
<beccari@dima.unipa.it>, <cammalleri@dima.unipa.it>, <sorge@dima.unipa.it>

ABSTRACT

The present work is articulated in two phases. Firstly, an extensive theoretical insight addresses the category of split-way CVT's, where V-belt mechanical variators are arranged inside complex drives including one or more epicyclic trains, in order to spread the output speed range as far as including neutral and reverse. All the arrangements are planned for the two-mode operation, where the switch from one mode to the other occurs in rotational synchronism of the connecting/disconnecting shafts. The most promising schemes are then selected basing on the concept of variator "class", aiming at the minimum variator size for fixed input power. In the second phase, the experimentation is carried out on each of the two modes of a particular drive prototype, recording torque and angular speed on the various branches in several operative conditions, in order to estimate the overall performance in terms of efficiency and power capacity. Simple and reliable formulas are proposed for the CVT efficiency in dependence on the various working conditions.

1. INTRODUCTION

It is known that the output speed range of a CVT can be widened by inserting the variator into double- or multi-way arrangements, where two or more branches are connected by epicyclic trains [1-7]. This practice can produce infinite or even negative "aperture" (ratio of maximum to minimum speed ratio) but is paid by an increase of the power demand to the variator, i. e. of its "class". By proper definitions of the "speed gain" and "power gain" of a complex CVT with respect to the simple variator, the principle of virtual displacements permits proving that the product of such two gains is equal to the unity in ideal no-friction conditions [1].

Previously, the behaviour of the double-way continuously variable drives with two epicyclic trains was recognised as completely defined by three "apertures": A of the whole drive speed ratio, A_1 of the variator driving speed, and A_v of the internal variator speed ratio. Once fixed these three numbers, the

single components may be suitably chosen in view of the simplest arrangements (for example, eliminating a gear, or an epicyclic train) [1-3]. Fixing only A and A_v, one degree of freedom is left (A_1), which can be used to minimise the variator class by controlling the compatibility of the power request with the capacity, at full input power.

The drawback of the variator class increase when enlarging the aperture A can be overcome by two- or multi-mode transmissions, where the switch from one mode to another is done by suitable clutches. The speed range can be substantially increased with a contained increase of the variator class, though at the cost of a more complex scheme [8, 9].

We want that the aperture changes from positive into negative, keeping its absolute value, by use of a two-mode CVT in place of the simple variator ($A = -A_v$). This means that the largest reverse speed is symmetrical with respect to the lowest original forward speed.

2. THEORY

2.1. Variator performance

Let us assume a V-belt variator, where pre-forcing is realised by means of an axial loading spring on the driven pulley, and consider ideal working conditions with no friction.

When the two half-pulley expand, the spring is compressed and thus the axial thrust decreases linearly with the winding radius (increases with the variator speed ratio τ_v), according to: $F_z = F_{z,min.}\{1 + (F_{z,max.}/F_{z,min.} - 1)[r_{DN,max.} - r_{DN}(\tau_v)] /(r_{DN,max.} - r_{DN,min.})\}$, where the subscript DN refers to the driven pulley. Moreover, the Euler-Grashof theory gives $F_z = (T_{DR} - qv^2)\,[(\Theta_{DN} - \theta_s)\, f_{eq.}\exp(-f_{eq.}\theta_s) + 1 - \exp(-f_{eq.}\theta_s)] / (2f_{eq.}\tan\alpha)$ (see [10]), where T_{DR} is the belt tension at the driver pulley entrance, qv^2 is the momentum flux (q = mass per unit length, v = belt velocity), $f_{eq.} = f / \sin\alpha$ is an equivalent coefficient of friction (α = groove half-angle), Θ_{DN} is the wrap angle over the driven pulley and θ_s is the sliding angular width over any of the two pulleys. Then, combining these results, we can put $F_{z,min.} = (T_{DR} - qv^2)\, Z(\theta_s, \tau_v)$, where $Z(\theta_s, \tau_v)$ is a function of the variables θ_s and τ_v.

Taking into consideration also the belt penetration due to side compression of the pulley walls, the axial thrust holds the same expression, but with a different functional dependence $Z(\theta_{s,DN}, \tau_v)$, where $\theta_{s,DN} \neq \theta_{s,DR}$ (see Ref. [11-13]). The sliding angle depends on the applied torque, while r_{DN} and Θ_{DN} are functions of τ_v, according with the well-known formulas, $\tau_v = r_{DR} / r_{DN}$, $r_{DN} - r_{DR} = D\sin\beta$, $L = 2D\cos\beta + r_{DR}(\pi - 2\beta) + r_{DN}(\pi + 2\beta)$, where D is the centre-distance, L is the belt length and 4β is equal to the driven wrap angle minus the driver one.

The Euler-Grashof model implies also the following relationship for the power

$$P_v = v\left(T_{DR} - qv^2\right)\left[1 - \exp\left(-f_{eq.}\theta_s\right)\right] = v\left(T_{DR} - qv^2\right)P(\theta_s) = v\,F_{z,min.}\,P/Z = v\,F_{z,min.}\,F(\theta_s,\,\tau_v) \tag{2.1}$$

Considering the radial penetration as well, the dimensionless function $P(\theta_s)$ is different from Eq. (2.1) and depends also on τ_v [1]. Nevertheless, whichever model is assumed for the belt-pulley interaction, the ratio P_v / $F_{z,min.}$ is equal to the belt velocity v times a function $F(\theta_{s,DN},\,\tau_v)$, independent of the variator class. The limit capacity of the variator is attained when the sliding angle grows as much as the wrap angle, or T_{DR} grows as much as the highest admissible tension. Reaching the two limits simultaneously should be the most convenient condition to be pursued. When working at both limits of tension and slip, P_v turns out to be a cubic function of the belt speed v.

Considering a series of geometrically similar variators, all realised with the same materials, the axial thrust $F_{z,min.}$ will be proportional to the square of the variator size, as any spring stiffness is proportional to the material shear modulus G times some linear size of the spring. Therefore, Equation (2.1) shows that $P_{v,max.}$ is proportional the third power of the variator size for constant input angular speed and then the volume can be assumed as a measure of the class.

The efficiency of a V-belt variator is mainly affected by the belt hysteresis losses while seating and unseating on the pulleys, which can be assumed independent of the applied torque, and by the slip losses, which increase with the transmitted torque. Other possible losses, attributable to the bearings, the air drag, some possible cascade gearing, etc., depend only on the input speed and on the speed ratio, but will be considered apart in the following. Therefore, the variator efficiency η_v may be roughly thought as given by the product of two factors:

$$\begin{aligned}\eta_v &= \eta_{slip}\,\eta_{seating\text{-}unseating} = (1 - c_{slip}\,M_{DR})(\,1 - c_{seating\text{-}unseating}\,/\,M_{DR}) = \\ &= a_0 - a_1\,M_{DR} - a_{-1}\,M_{DR}^{-1}\end{aligned} \tag{2.2}$$

where M_{DR} is the driving torque, while a_0, a_1 and a_{-1} are some loss coefficients to be determined by experiments. The coefficient c_{slip} increases on decreasing τ_v owing to the reciprocal dependence on the driver radius and to the radial penetration into the groove [14]: $1 - \eta_{slip} = (M_{DR}\,/r_{DR} + T_{DR}/k_{1,DR} - T_{DN}/k_{1,DN} - M_{DR0}\,/r_{DR} - T_{DR0}/k_{1,DR} + T_{DN0}/k_{1,DN}) / S_{long.}$, where $S_{long.}$ = longitudinal belt stiffness, $k_1 = k\,\tan(\alpha+\varphi)/\tan\alpha$, $k = 2\,\tan\alpha\,S_{transv.} / S_{long.}$ = V-belt elastic parameter, α = wedge half-angle, φ = friction angle and the subscript 0 refers to zero load. As the transverse stiffness $S_{transv.}$ is proportional to the square of the radius, also the penetration terms are influenced by the speed ratio.

2.2. Two-mode two-*ET* transmission

Suppose to split the speed range in two modes by an arrangement like in Fig. 1. The first mode uses the complete scheme, while the second blocks the relative motion of one *ET* and uses only the other. More generally, eight different two-mode CVT's could be generated by a scheme like this, according to which is the direction of the power flux, to which of the two *ET* is blocked and in which of the two modes.

With reference to the notation in Fig. 1, $\tau = \omega_B / \omega_A$, $\tau_v = \omega_b / \omega_a$ and $\tau_a = \omega_a / \omega_A$ indicate the speed ratio of the whole drive, of the variator and of the variator driving pulley to the input shaft. The quantities τ_{f1}, τ_{f2} and τ_{f3} are fixed speed ratios, to be considered in accordance with the arrow directions. Moreover, $\gamma_1 = M_2 / M_O$ and $\gamma_2 = M_4 / M_B$ indicate the ideal torque ratios on the correspondent *ET* shafts, where any torque is considered applied according to the arrows and is assumed positive if concordant with the rotation ω_A. It is possible to prove that γ_1 and γ_2 are constant, as they depend only on the internal speed ratios of the respective *ET* 's in the apparent motions relative to the carriers and on the specific shaft connections [6]. Fixing γ_1 and γ_2, the drive behaviour can be completely defined, independently of the inside configuration of the *ET* 's.

The scheme of Fig. 1 was preferred to the "symmetric" scheme of Ref. [1] because it permits simple and compact practical realisations: see the very fine example of Fig. 2, where the whole drive is realised with just two shaft lines. The external boxes enclosing the epicyclic trains rotate rigidly with their respective carriers and are connected by timing belts with the front shafts. One of the fixed ratio connections of Fig. 1 is absent in Fig. 2 ($\tau_{f3} = 1$).

The ideal power balance on the two *ET* permits to obtain τ_a and τ as functions of τ_v:

$$\tau_a(\tau_v) = \frac{\tau_{f1}}{\tau_{f1}(1-\gamma_1)+\tau_v\gamma_1} \tag{2.3}$$

$$\tau(\tau_v) = \tau_a(\tau_v)\tau_v\,\tau_{f3}\,\gamma_2 + \tau_{f2}\,(1-\gamma_2) \tag{2.4}$$

In these relationships, one has to replace $\gamma_i = 0$ or 1 when the correspondent *ET* is blocked and one branch is disconnected, because the torque on this branch vanishes.

The torque equilibrium at the nodes N_1 and N_2 permits calculating the ratio M_a / M_A, and the ideal power fraction P_v / P_A requested to the variator:

$$\frac{P_v}{P_A} = \tau_a(\tau_v)(1-\gamma_1)\left[1-\frac{\tau_{f2}(1-\gamma_2)}{\tau(\tau_v)}\right] \tag{2.5}$$

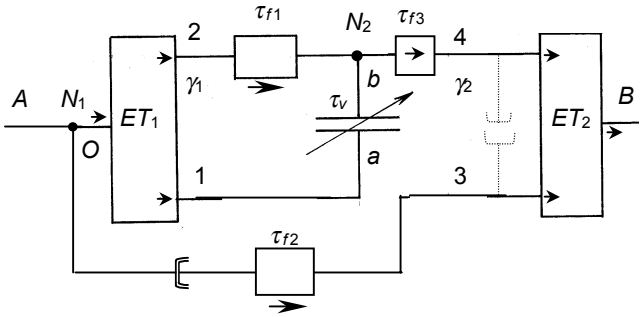

Figure 1. Two-mode split-way scheme.

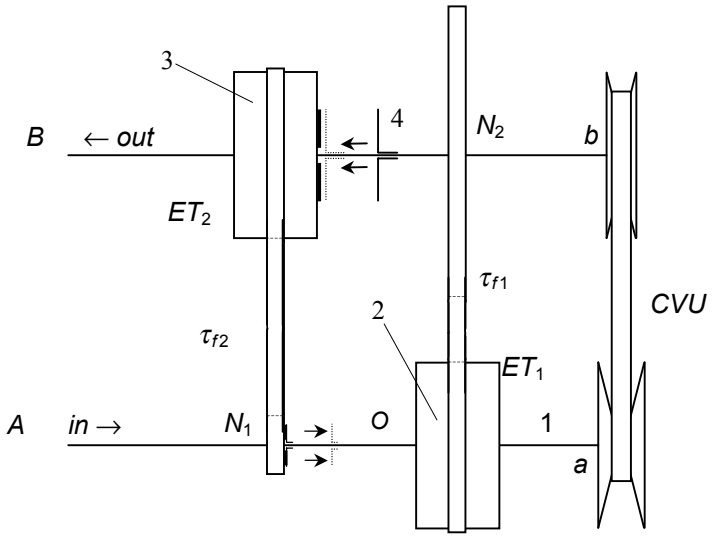

Figure 2. CVT component connection.
ET: epicyclic train, τ_f: timing belt speed ratio, *CVU*: continuously variable unit

On approaching the neutral, P_A tends to zero and the ideal ratio P_v / P_A diverges, i. e. some power circulation remains inside the drive. Of course, the real power input does not vanish due to the drive losses, but the whole nominal power cannot certainly be delivered. Therefore, some suitable device must be planned to cut the input power in some neighbourhood of the neutral, where then $P_{in} = P_{in,nominal}\ g(\tau)$ ($g(\tau) < 1$). For example, imposing the constancy of the ideal output torque within a symmetrical range spanning as far as τ_R yields $g(\tau) = 1$ for $\tau > -\tau_R$ and $g(\tau) = |\tau / \tau_R|$ for $\tau < -\tau_R$.

Referring the subscripts *R*, *N*, *S* and *F* to the largest reverse speed, the neutral, the switching point and the largest forward speed respectively, fixing τ_{vS}, the total drive aperture $A_{tot} = \tau_F / \tau_R$ and the variator aperture $A_v = \tau_{vS} / \tau_{vR}$ (> 1 or < 1, but > 0), five numbers are to be determined: τ_{f1}, τ_{f2}, τ_{f3}, γ_1

and γ_2. Introducing the first range fraction $A_I = \tau_S / \tau_R$ as a new parameter, two conditions derive from the correspondence between the partial apertures A_I and $A_{II} = A_{tot}/A_I$ with the changes A_v and $1/A_v$ of τ_v (the full range of τ_v is covered in either of the two opposite directions in each single mode). Adding the rotational synchronism constraint at the mode switching permits the calculation of the parameters in dependence on whichever three of them, for example γ_1, τ_{f2} and γ_2 as functions of A_I, τ_{f1} and τ_{f3}. Thus, three degrees of freedom are left at disposal for the variator class optimisation.

Consider Fig. 1 and assume that the complete scheme is used in the first mode, where τ_v decreases ($A_v < 1$), while ET_2 is blocked and the coupling τ_{f2} is disengaged in the second, where τ_v increases ($\tau_{vF} = \tau_{vS}/A_v > \tau_{vS}$). Putting $\gamma_2 = 1$ into Eq. (2.4) for the second mode, calculating τ at the extremes and putting $\tau_F/\tau_S = A_{tot}/A_I$, one obtains $\gamma_1 = \tau_{f1}(A_I - A_v A_{tot.}) / [\tau_{f1}(A_I - A_v A_{tot.}) + \tau_{vS}(A_{tot.} - A_I)]$.

Using Eq. (2.4) at the mode switching, the synchronism constraint gives $\tau_S = \tau_a(\tau_{vS})\tau_{vS}\tau_{f3}$ for $\gamma_2 = 1$, on the one hand, and $\tau_{f2} = \tau_a(\tau_{vS})\tau_{vS}\tau_{f3} = \tau_{f3}[\tau_{f1}(A_I - A_v A_{tot.}) + \tau_{vS}(A_{tot.} - A_I)] / [A_{tot.}(1 - A_v)]$ for $\gamma_2 \neq 1$, on the other hand.

As regards the first mode, calculate Eq. (2.4) at the range ends, $\tau_{vR} = \tau_{vS}/A_v$ and τ_{vS}, and obtain at last $\gamma_2 = (A_I - 1) / (A_I - A_{tot.})$.

2.3. Variator class

For constant input speed and power, the single way arrangement does not exploit the variator capacity at best over the whole range, as the admissible power is an increasing function of τ_v, and the condition closest to the full slip limit is reached at $\tau_{v,min.}$.

The evaluation of the variator class for a complex drive requires comparing with that particular variator that can deliver the same total power alone, at the same input speed and in condition of geometrical similitude. Indicating with stars $(...)^*$ the reference variator, the power ratio will be $P_v / P^*_v = P_v / P_{in,nominal} = g(\tau)\, P_v / P_{in}$. Minding the critical condition of the reference variator, we have $P_v / P_{in,nominal} = [\omega_{DR}\, r_{DR}\, F_{z,min.}\, F(\theta_s, \tau_v)] / [\omega_{in}\, r^*_{DR,min.}\, F^*_{z,min.}\, F(\theta_{s,max.}, \tau_{v,min.})]$ by Eq. (2.1) and observe that $(r_{DR,min.}\, F_{z,min.}) / (r^*_{DR,min.}\, F^*_{z,min.})$ equals the volumetric similitude ratio, i. e. the class C. Then, we get

$$C = \left[g(\tau) \frac{P_v}{P_{in}} \frac{\omega_{in}}{\omega_{DR}} \frac{r_{DR,min.}}{r_{DR}} \frac{F(\theta_{s,max.}, \tau_{v,min.})}{F(\theta_{s,max.}, \tau_v)} \right]_{maximum} \tag{2.6}$$

where P_v / P_{in} is given by Eq. (2.5). As $F(\theta_s, \tau_v)$ increases with θ_s, the limit value of F is used in the denominator of Eq. (2.6). Clearly, Eq. (2.6) will be satisfied just at one point of the speed range, while sub-critical conditions will be found elsewhere.

Basing on these concepts, all possible schemes like in Fig. 2 were analytically tested changing A_1 and τ_{f1} by tentative and calculating the other parameters like in the previous subsection (notice that $\tau_{f3} = 1$). Very good results are obtained for the case $\tau_{vS} = A_v = -1/A = 1/3.6$, when the first mode (two *ET*) covers the speed range $\tau_R < \tau < \approx -0.7\ \tau_R$ and the second the complementary range. In theory, the desired aperture increase can be obtained even with a small decrease of the variator class.

2.4. Efficiency

In the real operation with friction losses, the torque and torque ratios are indicated with overscored symbols ($\overline{M}_i$ and $\bar{\gamma}_i$). With reference to Figg. 1 and 2, the torque ratios can be calculated as in [3], $\bar{\gamma}_1 = \gamma_1 - (1 - \gamma_1)\ (\eta_1^{\mu_1} - 1)$, $\bar{\gamma}_2 = \gamma_2\ \eta_2^{\mu_2}$, where η_i are the *ET* apparent efficiencies in the motion relative to the carriers, $\mu_1 = \mathrm{sgn}[\overline{M}_O\,(\omega_{in} - \omega_2)]$ and $\mu_2 = \mathrm{sgn}[-\overline{M}_{out}\,(\omega_{out} - \omega_3)]$.

Imposing the torque equilibrium at the two nodes N_1 and N_2, one gets two different relationships for the ratio $\overline{M}_a / \overline{M}_{in}$, in dependence on the whole drive efficiency η, on the variator efficiency η_v and on the other parameters. This permits obtaining η, by elimination of $\overline{M}_a / \overline{M}_{in}$:

$$\eta = \frac{\left[\eta_v^{\mu_v}(1-\bar{\gamma}_1)\dfrac{\tau_{f1}}{\eta_{f1}^{\mu_{f1}}} + \bar{\gamma}_1\tau_v\right]\tau}{\dfrac{\tau_{f2}}{\eta_{f2}^{\mu_{f2}}}(1-\bar{\gamma}_2)\left[\eta_v^{\mu_v}(1-\bar{\gamma}_1)\dfrac{\tau_{f1}}{\eta_{f1}^{\mu_{f1}}} + \bar{\gamma}_1\tau_v\right] + \dfrac{\tau_{f1}}{\eta_{f1}^{\mu_{f1}}}\dfrac{\tau_{f3}}{\eta_{f3}^{\mu_{f3}}}\bar{\gamma}_2\tau_v} \tag{2.7}$$

where $\mu_v = \mathrm{sgn}(\overline{M}_a\,\omega_a)$, while η_{fi} are the efficiencies of the fixed ratio couplings and $\mu_{fi} = 1$ or -1 depending on the concordance or discordance of the power fluxes with the arrow directions.

3. EXPERIMENTS

The experimental prototype is shown in Fig. 3 a, b, c and is based on the scheme of Fig. 1. Owing to the limited choice of components available in the market (variator, epicyclic trains, etc.), some changes had to be made with respect to Fig. 2 and a third shaft line was added. Moreover, the fixed ratios are slightly different from the results by the previous theoretical procedure. Nevertheless, the drives of Fig. 2 and 3 are somehow equivalent as they both refer to the scheme in Fig. 1.

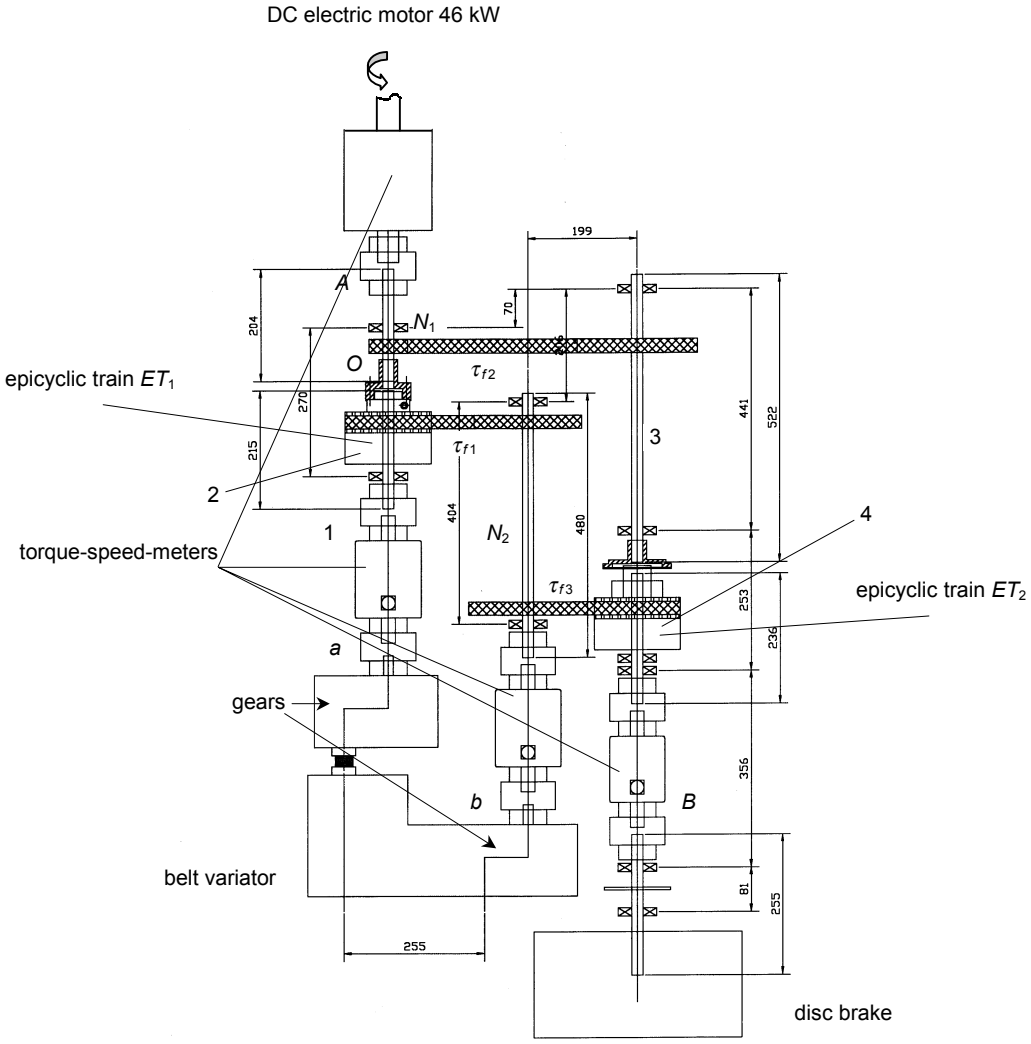

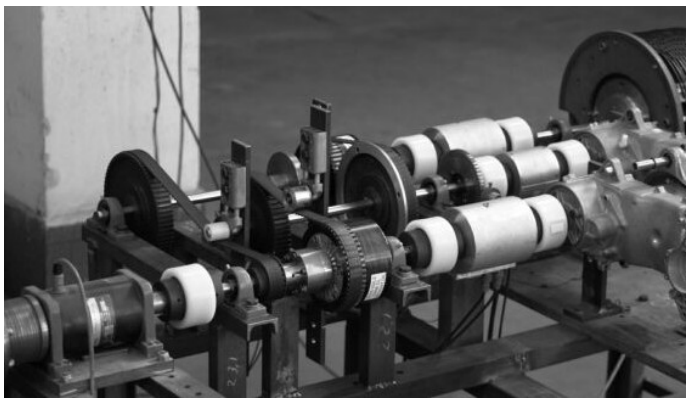

Figure 3 a, b, c. Experimental prototype.
a) Scheme of the arrangement. b) General view. c) Switching device.

It is remarkable that the power flux through the variator may flow in both directions *a*-*b* and *b*-*a*

depending on the particular speed ratio. This requires some attention in general when using a variator unsymmetrical with respect to the primary and secondary shaft.

A commercial variator is used for the experiments. Pre-forcing is realised by a loading spring on the right pulley of the scheme, which involves an increasing limit-power/speed-ratio characteristic diagram for constant input speed. Actually, the speed ratio is in reduction from *a* to *b* all over the range, due to the larger winding radii on the right pulley. This pulley is nearly always driven, save a power flux inversion in the range between the neutral and the mode switching, where thus the loading spring acts on the driver pulley, which condition is known as less efficacious as regards the belt tensioning [1, 12, 13]. Therefore, a lower power capacity of the variator should be expected in this range, where however, a possible remedy could consist in activating an extra spring in order to increase the axial thrust.

The variator is of the small size high speed type and permits delivering 2 kW approximately at 7500 rpm. The belt is cogged and has the following characteristics: width = 15 mm, thickness = 4 mm + cogs, length = 750 mm, wedge angle = 14°. Owing to the convenience of lower speeds for the remaining components of the transmission, two gear couplings were connected upstream and downstream of the variator, stepping up and down the speed respectively with ratios reciprocal of each other, and permitting to deliver a sufficient power level through the variable speed unit.

The power losses in these gears do not depend on the load but only on the working speed. They must be taken into consideration in the evaluation of the variator efficiency, when considering it as a single unit together with the end gears. With reference to the notation of Fig. 3 a, the torque directly applied to the inside driver pulley is $\overline{M}_a - \overline{M}_{a0}$ divided by the gear speed ratio, where $\overline{M}_{a0}$ is the lost torque in the upstream gearing, which was measured by experiments at several angular speeds, taking away the belt. Similarly, the torque directly applied to the inside driven pulley is $\overline{M}_b + \overline{M}_{b0}$ multiplied by the gear speed ratio. The diagrams of $\overline{M}_{a0}$ and $\overline{M}_{b0}$, in dependence on the rotation speed are reported in Fig. 4 a. A third degree polynomial interpolation of the experimental data gives a very good fit and can be used to build up a generalised experimental formula for the whole variator efficiency ($\overline{M}_i$ [Nm], n_i [rpm]):

$$\begin{aligned} \overline{M}_{a0} &= -0.08341 + 0.02915\, n_{a0} - 8.592 \times 10^{-5}\, {n_{a0}}^2 + 9.613 \times 10^{-8}\, {n_{a0}}^3 \\ \overline{M}_{b0} &= 1.133 + 0.001992\, n_{b0} - 1.1398 \times 10^{-5}\, {n_{b0}}^2 + 2.453 \times 10^{-8}\, {n_{b0}}^3 \end{aligned} \qquad (3.1\text{ a, b})$$

The variator was also tested alone in several running condition of speed and load, for the experimental calculation of the efficiency. Using these data and replacing M_{DR} with $\overline{M}_a - \overline{M}_{a0}$ into Eq. (2.2), such a linear-hyperbolic functional dependence proved to be quite suitable all over the

working field and the coefficients a_i were calculated by usual statistic procedures. Then, subtracting the losses in the gears and in the belt-pulley coupling from the input power, the following relationship can be derived at last for the whole variator efficiency, in place of Eq. (2.2)

$$\eta_v = \frac{-2.062 + 0.9\left(\overline{M}_a - \overline{M}_{a0}\right) - a_1\left(\overline{M}_a - \overline{M}_{a0}\right)^2 - \overline{M}_{b0}\tau_v}{\overline{M}_a} \tag{3.2}$$

where the coefficient a_1 depends on τ_v according to subsection 2.1. Putting $r_{DR} \cong 2r_1\tau_v/(1 + \tau_v)$, where r_1 is the wrap radius for $\tau_v = 1$, a good interpolation for the experimental results is given by the relationship

$$a_1 = c_{slip} = \frac{1 + \tau_v}{S_{long.}\left[2\,r_1\tau_v - b\left(1 + \tau_v\right)\right]} \tag{3.3}$$

where $r_1 = 0.0365$ m, $b = 0.0107$ m and $S_{long.} \cong 93000$ N. The agreement can be seen in Fig. 4 b.

Equation (3.2) holds also for the inverted power flux case, exchanging the subscripts *a* and *b* and replacing the ratio τ_v with $1/\tau_v$.

Figures 5 a, b, c show three example diagrams, in dependence on the torque applied on the upstream gearing. A very good fit can be observed between the results by Eqs. (3.1) to (3.3) and the

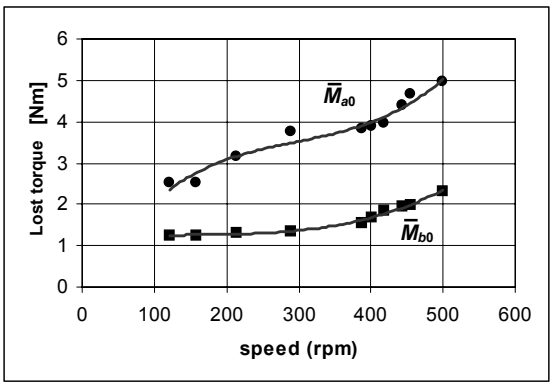

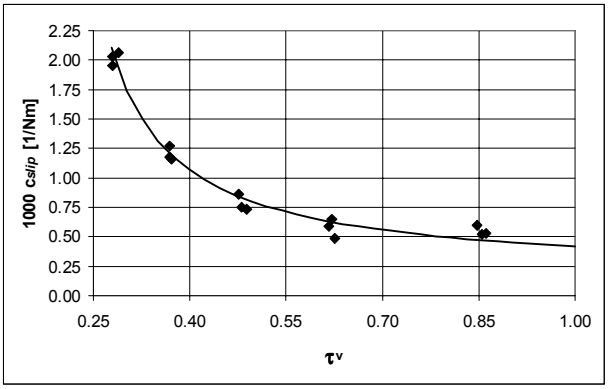

Figure 4.

a) Torque losses in the couplings upstream ($\overline{M}_{a0}$) and downstream ($\overline{M}_{b0}$) of the belt variator (continuous line: results by Eqs. (3.1 a, b)).
b) Belt slip coefficient versus variator speed ratio (continuous line: Eq. 3.3)).

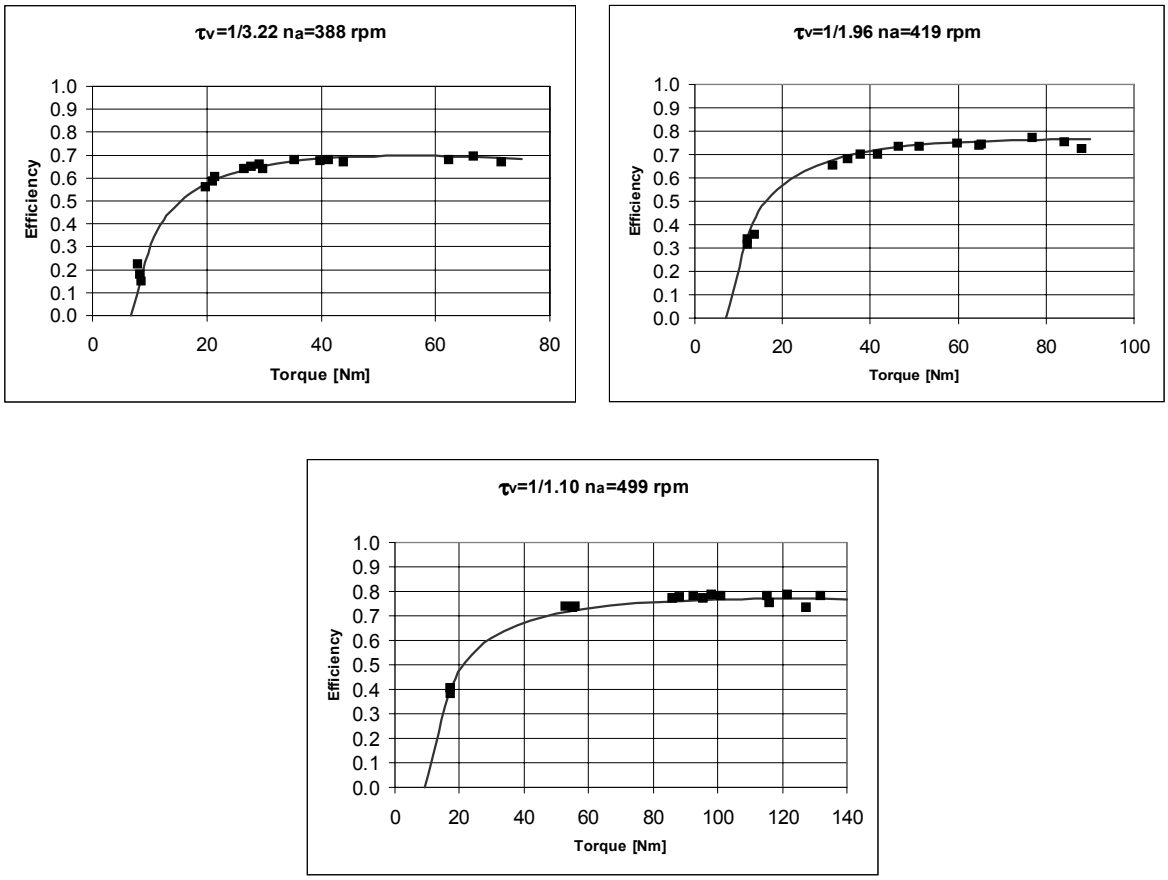

Figure 5 a, b, c. Variator efficiency versus input torque for several speed ratio (continuous line: results by Eqs. (3.1) to (3.3)).

experiments. Moreover, Equation (3.2) offers a simple tool for foreseeing the behaviour of the complex CVT set-up in the hypothesis of zero-losses in the gears or else in their absence.

Let us consider now the whole arrangement of Fig. 3 a, b. The second mode is obtained disconnecting the downstream epicyclic train ET_2 on the right from the upper shaft and blocking it by means of a splined bush with two external gears (Fig. 3 c), which rotates together with one of the *ET* wheels and can be engaged either with a coupling flange on the upper shaft or with the *ET* box on the lower side (i. e. with the carrier).

A DC electric motor of 46 kW drives the CVT and a disc brake, which is pneumatically operated, exerts an output torque ranging up to 288 Nm, though subject to the limitation of an admissible braking power of 3.5 kW. Four speed-torque meters of the strain-gauge type send their signals to suitable measurement units or else to oscilloscopes and the temperature of the gearbox oil is picked up by a thermocouple. The most significant data of the experimental prototype are reported hereafter

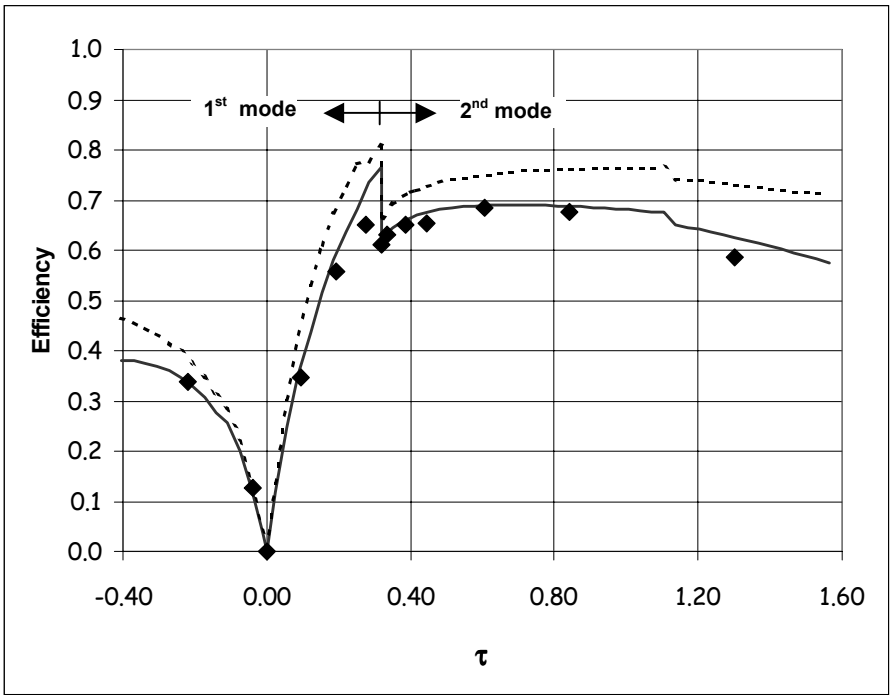

Figure 6. Efficiency of the prototype in the two operative modes
(lozenges: experimental values, continuous line: theoretical results by Eqs. (2.7) and (3.1) to (3.3), dashed line: theoretical results for $\overline{M}_{a0} = \overline{M}_{b0} = 0$).

τ_{f1}	τ_{f2}	τ_{f3}	γ_1	γ_2	A_I	$A_{tot.}$	$A_v = \tau_{vS}$	τ_R
51:65	23:72	72:51	− 0.353	− 0.581	− 0.792	− 3.877	1/3.6	− 0.403

Another difference from the scheme in Fig. 2 is that the downstream *ET* is connected to the variator exit through the carrier (4 in Fig. 3), and then the relationship between real and ideal torque is given by $\bar{\gamma}_i = \gamma_i - (1 - \gamma_i)\,(\eta_i^{\mu_i} - 1)$ for both *ET*'s, using the subscripts 1 or 2 and putting $\mu_1 = \text{sgn}[-\overline{M}_a\,(\omega_a - \omega_2)]$ and $\mu_2 = \text{sgn}[-\overline{M}_{out}\,(\omega_{out} - \omega_4)]$.

The following values were estimated for the efficiencies of the fixed ratio couplings: $\eta_1 = 0.96$, $\eta_2 = 0.98$, $\eta_{f1} = 0.98$, $\eta_{f2} = 0.99$, $\eta_{f3} = 0.98$. Moreover, it is remarkable that $\mu_{f1} = \mu_{f2} = -\mu_{f3} = -\mu_v$ over the whole speed range.

Extensive experimental tests were carried out on this prototype, measuring torque and angular speed in the various branches. The entrance and exit speed and torque on the variator gave its experimental efficiency. The theoretical efficiency of the variator and of the whole drive were obtained by Eq. (2.7) and Eqs. (3.1) to (3.3), where $\overline{M}_a$, η and η_v were calculated through an iterative

procedure using any one of the two equilibrium conditions at the nodes N_1 and N_2 that were mentioned in subsection 2.4., e. g.

$$\overline{M}_a = \overline{M}_{in}(1-\bar{\gamma}_1)\left[1-\frac{\tau_{f2}}{\eta_{f2}{}^{\mu_{f2}}}(1-\bar{\gamma}_2)\frac{\eta}{\tau}\right]$$

Figure 6 reports some experimental results. Observe the fine fit between theory and experiments. The efficiency decrease on increasing the speed ratio in the second mode is due to the increasing power through the variator, which is the less efficient component of the arrangement. This trend is associated with the chosen variation of τ_v, which decreases in the first mode and increases in the second, and could be overthrown by exchanging the speed ratio variation between the two modes, but at the cost of lower efficiency values towards the left side of the range. The abrupt change of the efficiency when switching from one mode to the other is due to the sudden increase/decrease of the power fraction through the variator and is also denounced by the experiments.

In the figure, a theoretical curve is also reported for the case without gearing, upstream and downstream of the belt variator. A substantial increase of the CVT efficiency can be obtained, which roughly indicates the limit performance that could be reached by this optimised hypothetical transmission.

ACKNOWLEDGEMENT

The authors acknowledge the Italian Ministry M.I.U.R. for the financial support to this research. They wish also to thank Mr. B. Drago, of the Department of Mechanics and Aeronautics, University of Palermo, for his helpful collaboration to the experimental work.

REFERENCES

[1] Sorge, F., Beccari, A. and Cammalleri, M., "Operative Variator Characterization for CVT Improvement", The JSME Intern. Confer. on Motion and Power Transmissions, Fukuoka, Japan, November 15-17, 2001.

[2] Sorge, F., "Present State and Future View of Research and Development of Transmission Belts and CVT in Italy", 2001 Intern. Seminar on Belt Transmission, Kyoto, Japan, November 19,

2001.

[3] Andolina, M. and Beccari, A., "Continuous Variation Transmission in Automotive Application: Extension of the Working Range of Automotive Transmission to Start and Reverse Motion with Minimization of Variator Dimension", The JSAE Intern. Conf. CVT '96, Yokohama, Japan, 1996.

[4] Beccari, A. and Sorge, F., "Experimental Results for a Variable Speed Differential Drive", 2nd British-Italian Workshop on Heat Engines, Bath, United Kingdom, 1991.

[5] Beccari, A. and Sorge, F., "Improved Performance of C.V. Transmissions for Passenger Cars", ATA, 3rd Intern. Conf. Innovation and Reliability in Automotive Design and Testing, Firenze, Italy, 1992.

[6] Beccari, A. and Sorge, F., "Trasmissione di Potenza con Variazione Continua del Rapporto di Trasmissione" (in Italian), ATA, Italy, v. 39, 1986.

[7] Beccari, A. and Cammalleri, M., "Semiautomatic Variator for Split Power CVT's", ATA Motor Car Engineering, Italy, December 2000.

[8] Beccari, A., "Schemi Bimodali Ottimizzati per la Trasmissione di Potenza con Due Vie in Parallelo e Rapporto di Trasmissione Variabile con Continuità" (in Italian), Internal Report, Institute of Machines, University of Palermo, Italy, 1997.

[9] Vahabzadeh, H., Macey, J. P. and Dittrich O., "A Split-Torque, Geared-Neutral Infinitely Variable Transmission Mechanism", SAE paper n. 905089, 1990.

[10] Beccari, A. and Cammalleri, M., "Implicit Regulation for Automotive Variators", Proceed. of Inst. of Mech. Engin., D6, v. 215, 2001.

[11] Sorge, F., "A Qualitative-Quantitative Approach to V-Belt Mechanics", ASME Journ. of Mech. Design, v. 118, 1996.

[12] Sorge, F., "A Simple Model for the Axial Thrust in V-Belt Drives", ASME Journ. of Mech. Design, v. 118, 1996.

[13] Gerbert, G., "Traction Belt Mechanics", Chalmers University of Technology, Göteborg, Sweden, 1999.

[14] Sorge, F., "Limit Performances of V-Belt Drives", CVT '99 Intern. Congress, Eindhoven, the Netherlands, 1999.

[15] Mantriota, G., "Theoretical and Experimental Study of a Power Split CVT System: Part I and II", Proceed. of Inst. of Mech. Engin., D7, v. 215, 2001.

[16] Mantriota, G., "Power Split CVT System with High Efficiency", Proceed. of Inst. of Mech. Engin., D3, v. 215, 2001.